Molecular simulations of outersphere reorganization energies for intramolecular electron and hole transfer in polar solvents

ARTICLE *in* CHEMICAL PHYSICS · DECEMBER 2005

Impact Factor: 1.65 · DOI: 10.1016/j.chemphys.2005.03.037

Available online at www.sciencedirect.com
SCIENCE DIRECT®
Chemical Physics 319 (2005) 4–15
Chemical Physics
www.elsevier.com/locate/chemphys

Molecular simulations of outersphere reorganization energies for intramolecular electron and hole transfer in polar solvents

I.V. Leontyev [a], A.V. Tovmash [a], M.V. Vener [a], I.V. Rostov [b], M.V. Basilevsky [a,*]

[a] *Karpov Institute of Physical Chemistry, ul. Vorontsovo Pole 10, Moscow 105064, Russia*
[b] *Supercomputer Facility, Australian National University, Canberra, ACT 0200, Australia*

Received 11 November 2004; accepted 24 March 2005
Available online 16 June 2005

Abstract

Outersphere reorganization energies (λ) for intramolecular electron transfer (ET) and hole transfer are studied in anion- and cation-radical forms of complex organic substrates (biphenylyl-spacer-naphtyl) in polar solvents simulated by means of the nonpolarizable models of water and 1,2-dichloroethane. The earlier elaborated molecular/continuum approach (the MD/FRCM, J. Chem. Phys., 119 (2003) 8024) is used; this method provides a physically relevant background for separating inertial and inertialess polarization responses within a nonpolarizable MD simulation (the SPC water model). Quantum-chemical calculations of solute charge distributions were performed with semiempirical (AM1) and second ab initio (HF/6-31G(d,p)) approximations. Ab initio charges give lower λ-values and are preferable, probably, because of including the effect of the SCRF polarization of the diabatic ET states. Standard Lennard–Jones and charge parameters implemented in MD runs were not specially fitted for reproducing ET effects. The difference in values for a cation and an anion originating from the same parent structure was specially investigated. As shown earlier, this effect, nonlinear in its nature, proved to be extremely large when a model dipolar two-site system was studied. For the present ET structures representing real chemical substrates it has reduced to a plausible value of 6–8 kcal/mol. The study of the temperature dependence of λ comprises a first MD simulation of this problem and its slope was found to be in accord with an experimental observation for an anionic species. Calculations of absolute λ-values for the hole transfer in 1,2-dichloroethane are the first MD simulations of reorganization energies in experimentally studied reactions. Computed values of λ-s are higher than the experimental data. The effect of this magnitude could be eliminated by proper tuning the solvent parameters.

Keywords: Electron transfer; Reorganization energy; Molecular dynamical simulation; Inertial polarization; Inertialess polarization

1. Introduction

Widely available and precisely elaborated methodologies in the theory of electrostatic solvation phenomena are based on continuum solvent models. Such computations of static equilibrium solvation effects are well described [1–5]. Applications of recent continuum theories for treating nonequilibrium solvation effects have also been reported. A solvation shell reorganization which accompanies charge redistribution processes in polar solvents comprises a typical example. Here the corresponding reorganization energy arises as a measure of the pertaining free energy barrier height [6]. Its computations for electron transfer (ET) reactions are conventionally performed in terms of the electrostatic continuum solvent approach [7–14] and reviewed elsewhere [15–17].

On the other hand, serious limitations are inherent to the continuum theory. Microscopic solvent description is required to treat the charge transfer in nonpolar solvents as well as for a proper account of temperature

* Corresponding author. Fax: +7 095 9752450.
E-mail address: basil@cc.nifhi.ac.ru (M.V. Basilevsky).

0301-0104/$ - see front matter © 2005 Elsevier B.V. All rights reserved.
doi:10.1016/j.chemphys.2005.03.037

trends in reorganization energies [16–19]. Additionally, nonlinear effects, missing in conventional versions of the continuum theory, may sometimes be important. Circumventing these limitations is especially important for biological applications where the deficiency of a macroscopic concept of a continuum medium becomes obvious being addressed to biological macromolecules. Several attempts of treating ET reorganization energies for more or less simple solutes modeling such systems at a molecular level based on MD simulations have been reported during the last decade [20–22]. The alternative molecular level techniques implementing the integral equations of statistical mechanics (the RISM theory) have been also considered recently [23]. All these treatments were performed in the framework of nonpolarizable solvent models. Neglect of the polarization of medium electrons by the electric field created by the solute charge distribution is a common deficiency of such approaches. For instance, as applied to ET, a separation of the electronic (inertialess) polarization component from the total polarization response is necessarily required. In continuum theories this problem is resolved by invoking two phenomenological parameters: the static (ε_0) and optical (ε_∞) dielectric permittivities, which were combined in the so-called Pekar factor:

$$C = (1/\varepsilon_\infty - 1/\varepsilon_0), \tag{1}$$

in earlier most simplistic theories [6,24] and operated in a more sophisticated way in the recent approaches that explicitly account for the excluded volume effect [7–12].

Medium structure can also be considered explicitly in terms of the nonlocal electrostatic theory [25–27], the most refined version of the dielectric continuum approach. Computations are exact for spherically symmetric systems [28,29], but as applied to the ET problem only approximate two-sphere (dumbbell) model of a solute is available [25,36,30,31]. Attempts of solving three-dimensional nonlocal electrostatic equations [29,32] have never been reported. This route could hardly provide any computational advantage over straightforward molecular simulations, the latter being conceptually more simple and transparent.

Within molecular simulation, only polarizable solvent models are capable of separating explicitly the electronic polarization field. Recent computational algorithms [33–37] based on earlier theoretical models [38–44] are now elaborated. Being computationally costly, these techniques have never been applied to treat real ET systems or even their simple molecular analogues, although computations for the oversimplified two-site ET model have been published [45].

In the preceding work [46] a physically relevant prescription for a separation of the inertial (nuclear) and inertialess (electronic) medium responses has been formulated in terms of standard nonpolarizable MD simulations. It was tested for equilibrium solvation energies of polyatomic ionic solutes producing a satisfactory agreement with the experiment [47]. Reorganization in a two-site ET model has been also considered [46]; this study has revealed a new nonlinear effect missing in continuum theories. In the present article we extend this approach to treat outersphere reorganization energies in real intramolecular ET systems. The presence of the above-mentioned nonlinear effect is confirmed and a reliable estimate of its magnitude is obtained. Additionally, the temperature dependence of reorganization energies is studied at a molecular level. The studies were performed using water as a model polar solvent, common for both cationic and anionic solutes. Computations were also extended for 1,2-dichloroethane (DCE); they simulated hole transfer for real ET substrates in a real solvent for the systems studied experimentally.

The corresponding methodological background is briefly reviewed in Section 2. Section 3 formulates its computational realization for reorganization energies. The results of computations are summarized and discussed in Sections 4 and 5 and concluded in Section 6.

2. Outline of the MD/FRCM method

2.1. Motivation

The inertialess response field arises due to the polarization of solvent electrons by a solute charge distribution. At a molecular level, this effect is tractable in terms of polarizable MD simulations [33–37]. Here the electronic polarization is treated classically which is legitimate owing to a large discrepancy between electronic and nuclear characteristic timescales. The average impact of medium electrons on nuclear dynamics is consistently captured by such approach. Even with this simplification, polarizable molecular level simulations require much larger computational effort than conventional nonpolarizable schemes.

The problem of separating the electronic (inertialess) polarization has been successfully solved in continuum ET theories [6,24] by the introduction of Pekar factor (1). The optical dielectric permittivity ε_∞ entering this equation cannot naturally appear in those molecular simulations which fully neglect the electronic structure of a solvent. Our refined molecular level approach accounts for the electronic polarization by explicit incorporation of ε_∞ in its computational scheme and a resulting renormalization of the effective solvent charges and their response field. In a MD computation of solvent configurations equilibrated to the total (electrostatic + nonelectrostatic) solute force field all electrostatic interactions are scaled by the factor $1/\varepsilon_\infty$ (Eq. (4) below). In this way the inertial polarization

component is determined. The complementary inertialess component (i.e. the electronic response to the solute electric field, constituting an essential part of the total response) is considered by means of a continuum approach and next added to the inertial component found at a molecular level. This description follows in the linear response approximation as a result of strongly distinguishing relaxation periods for inertial and inertialess polarization fields. It was originally formulated by Dogonadze, Kornyshev and Kuznetsov [27]. In this way, the basic idea, borrowed from the continuum ET theory, is implemented in the present work in the context of a combined molecular/continuum treatment of polar solvents.

This model, called MD/FRCM [46,47], combines a nonpolarizable MD simulation with the continuum FRCM scheme (the Frequency Resolved Cavity Model, using frequency resolved cavity for the solute excluded volume [12,15]). The discrete solvent particles with average dipoles $\bar{\mu}$ and the corresponding point charges $\bar{q}_v(\sum_\mu \bar{q}_\mu = 0)$ are immersed in the medium modeled as a continuum with dielectric permittivity $\varepsilon = \varepsilon_\infty$. Quantities $\bar{q}_\mu$ represent mean solvent charges in the bulk. As shown in Fig. 1, this picture is complemented by inserting at the center of the MD cell a solute molecule, with atomic point charges q_I, considered as nonpolarizable in the present most simple version). Nonelectrostatic intermolecular forces are conventionally described by pairwise Lennard–Jones (LJ) interactions.

2.2. Renormalization of charges

The electrostatic forces are monitored by the solute charge density

$$\rho^{\mathrm{slt}} = \sum_i q_i \delta(r - r_i), \tag{2}$$

and the similar solvent counterpart

$$\rho^{\mathrm{slv}} = \sum_\mu \bar{q}_\mu \delta(r - r_\mu), \tag{3}$$

where r_i and r_μ denote the points where the corresponding charges are located.

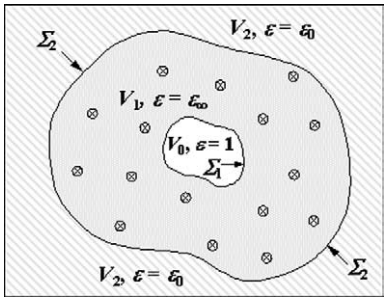

Fig. 1. Illustration of the MD/FRCM computations.

The electronic continuum is bounded from inside by the solute region with $\varepsilon = 1$ having volume V_0 and surrounded by the boundary surface Σ_1. It is also necessary to introduce the external continuum with static dielectric permittivity ε_0. It fills the external volume V_2 outside the second boundary surface Σ_2. The region V_1 with $\varepsilon = \varepsilon_\infty$, where discrete solvent particles are explicitly considered, is contained between surfaces Σ_1 and Σ_2. Introducing the external region is a complication arising, due to long-range Coulomb interactions, as a purely technical problem of getting a reasonably fast converging computational procedure.

The peculiarity of the present treatment is performing all electrostatic computations with scaled solute and solvent charges. The corresponding Coulomb interactions are:

$$\frac{q_i^{\mathrm{eff}} q_v^{\mathrm{eff}}}{r_{iv}} \ (\text{solute/solvent}) \text{ and } \frac{q_\mu^{\mathrm{eff}} q_v^{\mathrm{eff}}}{r_{\mu v}} (\text{solvent/solvent}), \tag{4}$$

where $r_{\mu v} = |r_\mu - r_v|$ and $r_{iv} = |r_i - r_v|$. The effective charges are related to the real ones introduced in Eqs. (2) and (3) as

$$q_\mu^{\mathrm{eff}} = \frac{\bar{q}_\mu}{\sqrt{\varepsilon_\infty}}; \quad q_i^{\mathrm{eff}} = \frac{q_i}{\sqrt{\varepsilon_\infty}}. \tag{5}$$

The charges q_μ^{eff} can be borrowed from any particular nonpolarizable simulation scheme, for instance, from the SPC water model [48]. Solute charges q_i are obtained in quantum-chemical computations. Scaling charges in Eq. (5) can be reformulated in terms of renormalized interactions

$$\frac{\bar{q}_\mu \bar{q}_v}{\varepsilon_\infty r_{\mu v}} \ (\text{solvent/solvent}) \text{ and } \frac{q_i \bar{q}_v}{\varepsilon_\infty r_{iv}} \ (\text{solute/solvent}). \tag{6}$$

These laws follow immediately for the case where relaxation timescales for electronic and nuclear motions are strongly separated under additional constraints of linear and local response for electronic polarization modes [27,46]. Interactions (4) and (6) become identical provided the scaling of charges suggested by Eq. (5) is accepted.

2.3. The computational scheme

A combination of charge distributions (2) and (3), together with the continuum dielectric scheme illustrated by Fig. 1, results, in the linear response approximation, in the following expression for the mean response field of the solvent:

$$\Phi(r) = \Phi^{\mathrm{d}}(r) + \Phi^{\mathrm{c}}(r). \tag{7}$$

The first term, called the "direct response field" is the electrostatic potential created by the discrete solvent particles occupying region V_1,

$$\Phi^{\mathrm{d}}(r) = \left\langle \sum_{\mu} \frac{\bar{q}_{\mu}}{\varepsilon_{\infty}} \frac{1}{|r - r_{\mu}|} \right\rangle_{\rho,T}. \tag{8}$$

The average is performed over the equilibrium ensemble of solvent configurations found in the above described MD simulation with scaled Coulomb interactions. It is equilibrated to the solute charge distribution $\rho = \rho_{\mathrm{slt}}$. The second term in Eq. (6), called the "continuum response field", represents a response of the two dielectric continua, those filling volumes V_1 and V_2, to the electric solute charge (2). It is available by solving Poisson equation which includes both charge distributions ρ^{slt} and ρ^{slv} with proper matching conditions for boundaries Σ_1 and Σ_2. This approach was elaborated earlier and called "FRCM procedure" [12]. Its present version differs from the original purely continuum formulation by adding explicit solvent charges of ρ^{slv} and strongly extending the intermediate layer (with volume V_1) where these charges are contained. The external boundary is now shifted as far as possible apart from the solute region in order to provide the most realistic molecular structure of the solvent in the region V_1. In the earlier formulation this region represented only the first solvation shell with solvent molecules treated implicitly.

In Eq. (7) a polarization of the continua in both regions V_1 and V_2 by solvent charges (3) is neglected. Its smallness has been verified earlier [46]. With this reservation, Eq. (7) represents the total medium response. Finally, in order to complete the desired separation of its inertial component, it suffices to repeat the procedure implemented in the FRCM method [12]:

$$\Phi^{\mathrm{in}}(r) = \Phi^{\mathrm{d}}(r) + \Phi^{\mathrm{c}}(r) - \Phi^{\infty}(r), \tag{9}$$

where the inertialess response $\Phi^{\infty}(r)$ is found within the conventional Polarizable Cavity Model (PCM) scheme [1,3], and we have to take $\varepsilon = \varepsilon_{\infty}$ in the whole space outside the solute boundary Σ_1.

3. Computations of solvent reorganization energies

3.1. The general formulation

Consider two charge distributions of a solute, $\rho_{\mathrm{I}}(r)$ and $\rho_{\mathrm{II}}(r)$ corresponding to the initial and final states of the intramolecular ET process. According to Eq. (2), they are specified as two arrays of point charges q_{i}. The corresponding equilibrium response fields are obtained as:

$$\Phi_{\mathrm{I}} = \hat{K}_{\mathrm{I}}\rho_{\mathrm{I}}; \quad \Phi_{\mathrm{II}} = \hat{K}_{\mathrm{II}}\rho_{\mathrm{II}}. \tag{10}$$

The response operators $\hat{K}_{\mathrm{I}}$ and $\hat{K}_{\mathrm{II}}$ actually reformulate, as clarified below, computational schemes described in Section 2. In Eq. (10) both fields Φ_{I} and Φ_{II} and operators $\hat{K}_{\mathrm{I}}$ and $\hat{K}_{\mathrm{II}}$ are assumed to be inertial, i.e. we use a contracted notation $\Phi_{\mathrm{in}} = \Phi_{\mathrm{total}} - \Phi^{\infty} \to \Phi$ and $\hat{K}^{\mathrm{in}} = \hat{K}^{\mathrm{total}} - \hat{K}^{\infty} \to \hat{K}$, where subscript "in" is suppressed. Originally, Φ and $\hat{K}$ stand for the total response quantities whereas Φ^{∞} and $\hat{K}^{\infty}$ are their inertialess counterparts. The basic original operators $\hat{K}$ and $\hat{K}^{\infty}$ denote, within a shorthand notation, the procedure of obtaining, respectively, the total field $\Phi(r)$ (MD/FRCM, Eq. (6)) and the inertialess field $\Phi^{\infty}(r)$ (PCM, Eq. (9)) as described above. The inertial operators $\hat{K}$ in Eq. (10) are supplied by subscripts I and II because such response operators are generally ρ-dependent [46,49]. In this general nonlinear case we can find by means of thermodynamic integration the equilibrium solvation free energies ΔF_{I} and ΔF_{II} for states I and II; then electrostatic nonequilibrium free energies are defined within harmonic approximation as:

$$\begin{aligned} \Delta F[\Phi|\rho_{\mathrm{I}}] &= \Delta F_{\mathrm{I}} - \frac{1}{2}\left\langle \Phi - \Phi_{\mathrm{I}} \middle| \hat{K}_{\mathrm{I}}^{-1} \middle| \Phi - \Phi_{\mathrm{I}} \right\rangle, \\ \Delta F[\Phi|\rho_{\mathrm{II}}] &= \Delta F_{\mathrm{II}} - \frac{1}{2}\left\langle \Phi - \Phi_{\mathrm{II}} \middle| \hat{K}_{\mathrm{II}}^{-1} \middle| \Phi - \Phi_{\mathrm{II}} \right\rangle. \end{aligned} \tag{11}$$

The bracket notation means integrations over r or scalar products. Fields $\Phi - \Phi_{\mathrm{I}}$ and $\Phi - \Phi_{\mathrm{II}}$ denote deviations of solvent coordinate Φ from its equilibrium positions. (Note that operators $\hat{K}$ are negatively definite [40]). The reorganization energies for the direct (I → II) and the reverse (II → I) processes are denoted as λ_{I} and λ_{II}, respectively. They are obtained [36] by inserting $\Phi = \Phi_{\mathrm{II}}$ in the first line of Eq. (11) and $\Phi = \Phi_{\mathrm{I}}$ in its second line. They become equal in a purely linear case when $\hat{K}$ is ρ-independent: $\hat{K}_{\mathrm{I}} = \hat{K}_{\mathrm{II}} = \hat{K}$ and $\lambda_{\mathrm{I}} = \lambda_{\mathrm{II}} = \lambda$. Then a conventional Marcus equation for the ET barrier height arises [6]. This becomes invalid if $\lambda_{\mathrm{I}} \neq \lambda_{\mathrm{II}}$ but, provided the discrepancy is small $\left(\left|\frac{\lambda_{\mathrm{II}} - \lambda_{\mathrm{I}}}{\lambda_{\mathrm{I}}}\right| \ll 1\right)$, such a prescription still remains a reasonable approximation after assuming $\lambda = \frac{1}{2}(\lambda_{\mathrm{I}} + \lambda_{\mathrm{II}})$. This approach, invoked in the present work, results in [46]

$$\begin{aligned} \lambda &\approx \frac{1}{2}(\lambda_{\mathrm{I}} + \lambda_{\mathrm{II}}) \\ &\approx \frac{1}{2}\{\langle\rho_{\mathrm{I}}|\Phi_{\mathrm{I}}\rangle + \langle\rho_{\mathrm{II}}|\Phi_{\mathrm{II}}\rangle - \langle\rho_{\mathrm{I}}|\Phi_{\mathrm{II}}\rangle - \langle\rho_{\mathrm{II}}|\Phi_{\mathrm{I}}\rangle\}, \end{aligned} \tag{12}$$

where $\langle\ldots\rangle$means integration over r.

Provided operators $\hat{K}$ do not depend on ρ, a standard expression [6,7] arises from Eq. (12), namely

$$\begin{aligned} \lambda &= \frac{1}{2}(T_{\mathrm{I\,I}} + T_{\mathrm{II\,II}} - 2T_{\mathrm{I\,II}}), \\ T_{ab} &= -\int \mathrm{d}^3 r \rho_a(r)\Phi_b(r) = -\langle\rho_a|\hat{K}|\rho_b\rangle. \end{aligned} \tag{13}$$

Here, $T_{ab}(a, b = \mathrm{I}, \mathrm{II})$ are elements of the so called reorganization matrix.

3.2. The computational algorithm

When solute charge distributions are treated as collections of point charges, all functions and integrals reduce, respectively, to vector-arrays and sums representing their scalar products. The computation of the reorganization energy is then performed in the following sequence.

(a) A quantum-chemical computation of the charge distributions ρ_{I} and ρ_{II} for the ET states. We tested both semiempirical and ab initio methods and the methodologies required proved to be different for these two cases, see below.
(b) Finding the statistical ensembles of solvent molecular configurations that are equilibrated, respectively, to ρ_{I} and ρ_{II}. This was done by means of the MD simulations that scaled electrostatic interactions (4) and (5) as discussed in Section 2 with the solute charges q_i and solvent charges q_v^{eff} corresponding to the SPC water model [48].
(c) The MD trajectories from step (b) were inserted in the averaging procedure for a computation of direct field arrays $\Phi_a^{\mathrm{d}}(r_i), a = \mathrm{I}, \mathrm{II}$, where r_i denote positions of the solute atoms.
(d) A FRCM computation gives the arrays of continuum inertialess fields $\Phi_a^{\mathrm{c}}(r_i), a = \mathrm{I}, \mathrm{II}$.
(e) A PCM computation produces the inertialess continuum arrays $\Phi_a^{\infty}(r_i), a = \mathrm{I}, \mathrm{II}$. The inertial field arrays are then available from Eq. (9).
(f) The reorganization energy is evaluated following Eq. (12) where integrals $\langle \ldots \rangle$ are interpreted as scalar products over charge and field arrays.

3.3. The ET systems

We considered intramolecular ET in biphenylyl/naphthyl donor–acceptor systems with a rigid hydrocarbon bridge connecting donor and acceptor fragments. Two particular systems investigated below are

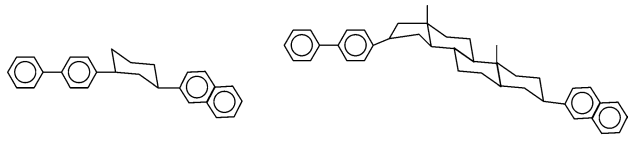

System A System B

The biphenyl fragment serves as a donor and the naphtalene fragment is an acceptor. Ion-radical forms of A and B have been studied with charges –1 (the electron transfer) or +1 (the hole transfer). The cation-radicals were also considered in the form of the so-called "anti-anion" (see Section 4.1). Experimental reorganization energies for intramolecular ET in tetrahydrofurane and for hole transfer in 1,2-dichloroethane in these systems are known [50–52]. Continuum (FRCM) computations have been reported earlier for the series of such ET systems [12] and most stable conformations established in this work were used.

3.4. The solute charge distributions

3.4.1. Semiempirical calculations

In this case the ET states were defined as CI 2×2 wave functions [7,9,12]. The key point is to select the orbital basis for constructing the two Slater determinants corresponding to the charge location on the donor and acceptor fragments. It is supposed that this basis is common for both states (i.e. the MOs are the eigenfunctions of a common Hamiltonian) which are therefore orthogonal.

The experience of earlier continuum computations showed that, in the case of ion-radicals, using canonical HF orbitals is not advisable. The charge localization on one or the other end of the molecular system results in adjusting all MOs to this biased charge distribution. The CI SCF procedure converges (as a result of its nonlinearity) to two different solutions, corresponding either to a donor or to an acceptor state with different charge distributions [53]. This effect increases when the medium reaction field is included in the Hamiltonian in terms of the SCRF procedure. The resulting solutions represent two Hamiltonians with different solvent response fields. As a net result, the desired MO basis set, universally describing both donor and acceptor states, cannot be obtained. Appropriate orbitals are, however, available from a HF treatment of closed shell systems, the counterparts of a given ion-radical, obtained by either adding one electron or its elimination [7,9]. For a consistent description, these two options must give a similar final result (i.e. the same reorganization energy), which should be specially verified. The corresponding closed-shell systems are less polarizable than their parent ion-radicals and invoking vacuum or solvent-modified orbitals does not make a significant difference. Computationally, vacuum orbitals are more convenient and they were utilized in getting the results listed below. Semiempirical AM1 parametrization was always used for computing geometries and charges.

3.4.2. Ab initio calculations

In present work, ab initio methods were employed to obtain geometry and atomic charge distribution for reactant and product states for treated ET systems. We used GAUSSIAN-03 [54] for ab initio calculations. As mentioned earlier, we considered the outer-sphere reorganization effects on fixed geometry. This geometry must not be favorable to either of the strong-localized

ion-radical ET states. As such, we used geometry obtained after optimization of the neutral delocalized system in vacuo. This geometry was computed at the HF/6-31G(d,p) level for systems A and B. Atomic point charge distributions for reactant and product states of both anion-radical and cation-radical ET systems A and B were calculated employing the SCRF-PCM method at the ROHF/6-31G(d,p) level followed by the ESP [55] procedure of fitting atomic charges to reproduce electrostatic potential of the considered system. Later, these sets of atomic point charges were used as solute charge distributions ρ_{I} and ρ_{II}. Dielectric constant used in the SCRF-PCM calculations was $\varepsilon = 7.58$ in case of anions and $\varepsilon = 10.36$ in case of cations. These values correspond to tetrahydrofurane and 1,2-dicloroethane (DCE) solvents, respectively (the solvents in which the corresponding λ's were experimentally studied [50–52]).

In order to obtain two SCF solutions with different charge localization of resulted wavefunction, we have to ensure at the beginning of calculation that the proper spin-orbitals corresponding to either of ET states are included in the Slater determinant. It can be obtained by altering the order of MOs in initial guess for SCF wavefunction using the Guess = Alter keyword in the GAUSSIAN-03. For example, the default guess for SCF wavefunction brings the final solution for anion-radical of system B to the product state of the ET reaction, with charge localized on acceptor. However, switching the order of MOs in initial guess between 147 (HOMO, acceptor localized) and 148 (LUMO, donor localized) gives the SCF solution corresponding to the reactant state of the ET reaction with charge localized on donor. The presence of solvent polarization field helps to stabilize the SCF solution of the required charge localization. Without it, as in analogous in vacuo ROHF or UHF calculations of the treated ET systems, the SCF procedure was falling into the same single solution with lower energy, corresponding to the product state in the considered case, despite of differences in initial guess of the active space.

By this means, the solute polarization by the solvent field was taken into account. However, the so obtained two SCF solutions are built with two different SCRF solvent potentials and are, therefore, nonorthogonal (but they were orthogonal in semiempirical calculations). This was disregarded in the present work. The nonorthogonality corrections in charge distributions, proportional to the square of the overlap integral between the two diabatic ET states, were neglected. This approximation is legitimate for calculating reorganization energies when donor and acceptor states are well spatially separated (the nonadiabatic ET) as for systems A and B.

3.5. The MD simulations in water

The GROMOS-96 package [56] was used. The computational scheme, described earlier [46], was based on SPC water model and implemented the reaction field (RF) technique for treating long range Coulomb sums, $\varepsilon_{\mathrm{RF}} = 70$ [57]. All computations were performed with a rectangular cell. In the case of system A, the cell contained 2160 water molecules, the values of its edges being approximately 35.8, 37.9 and 47.9 Å. In the case of system B, the cell contained 2420 water molecules, the values of its edges being approximately 35.8, 36.9 and 55.4 Å. The ultimate size of the equilibrium cells was established based on a preceding NPT computation (pressure = 1 bar, $T = 300$ K). The isothermal compressibility of water equals to 45.91 10^{-6} Bar^{-1} [56]. The solutes were rigid and fixed at the origin. All point charges, including those of H atoms, were explicitly counted. On the other hand, when LJ interactions were considered, we used the GROMOS atomic group parametrization in which hydrogen atoms were suppressed. So the different carbon groups are: (C, no hydrogen atoms attached), aliphatic CH (CH1), aliphatic CH_2 (CH2), CH_3 (CH3) and aromatic CH (CR1), where symbols in brackets indicate the atomic code. In the case of system A the geometry computed at the AM1 level was used in the MD simulations. (This enables us to estimate the influence of the partial charge definition on the computed λ values, see Section 4.1).

The coupling constant with the Berendsen thermostat was 0.3 fs. The isotropic pressure scaling option was used, the coupling parameter with the Berendsen barostat being 0.4 fs. The trajectory step size was 2 fs and the pairlist was updated after every 3 steps. The cutoff radii were 15 Å. A preliminary equilibration step for every trajectory was performed during 100 ps. The following main step with the length 400 ps produced the set of equilibrium solvent configurations.

For a given MD trajectory, the electrostatic interactions have been treated as described in Section 2. The parameters of the MD/FRCM procedure were $\varepsilon_\infty = 1.78$ and $\varepsilon_0 = 78.39$; the cavity parameter was $\kappa = 0.9$. This last parameter scaled (according to the PCM procedure [1,3]) effective atomic radii (R_1) of the solute atoms used to construct the internal cavity with the surface Σ_1 (Fig. 1): $R_1 = \kappa R_{\mathrm{vdW}}$. Here R_{vdW} is the van der Waals radius of a particular solute atom determined from its LJ potential with the GROMOS parametrization [56]. Effective atomic radii of the solute atoms used to construct the external cavity with the surface Σ_2 (Fig. 1) equal to 15 Å for all atoms.

3.6. The MD simulations in 1,2-dichloroethane

The GROMACS package [58,59] with the nonpolarizable model of DCE [60] has been used. All computations were performed with a rectangular cell. In the case of system A, the cell contained 958 DCE molecules, the values of its edges being approximately 50.0, 50.0 and 50.0 Å. In the case of system B, the cell contained

1146 DCE molecules, the values of its edges being 50.0, 50.0 and 60.0 Å. The solutes were rigid and fixed at the origin. All point charges, including those of H atoms, were explicitly counted. On the other hand, when LJ interactions were considered, we used the GROMACS atomic group parametrization in which hydrogen atoms were suppressed. So the different carbon groups of a solute were the same as in the case of water solvent (Section 3.5) and GROMOS computations. It should be noted that the LJ parameters of the C and CR1 groups are the same in the GROMOS [56] and GROMACS [58,59] force fields. Density of solvent equals to 1.23 g/cm^3 [60] for the considered cells.

The coupling constant with the Berendsen thermostat was 0.3 fs and $T = 300$ K (the NVT ensemble). The trajectory step size was 2 fs and the pairlist was updated after every 3 steps. The RF technique was used for treating the long-range Coulomb sums, cutoff radius was 15 Å and $\varepsilon_{RF} = \varepsilon_0/\varepsilon_\infty = 5$. (Implementation of the MD/FRCM involves two dielectric constants ε_∞ and ε_0, whereas the RF option in GROMACS allows using only a single dielectric constant ε_{RF}. It can be shown that setting $\varepsilon_{RF} = \varepsilon_0/\varepsilon_\infty$ is an adequate approach for the present case). The preliminary equilibration step for every trajectory was performed during 100 ps. The following main step produced the set of equilibrium solvent configurations.

For a given MD trajectory, the electrostatic interactions have been treated as described in Section 2. The parameters of the MD/FRCM procedure were $\varepsilon_\infty = 2.08$ and $\varepsilon_0 = 10.4$; the cavities parameters were described in Section 3.5.

4. Intramolecular ET and hole transfer in water

4.1. ET in anions and cations

We considered anionic (electron transfer) and cationic (hole transfer) forms of structures A and B in water solvent. Different reorganization energies for electron and hole transfers in a model dipolar two-site solute in water have been revealed and interpreted earlier [46]. The effect arises only within a molecular calculation; it is caused by the ρ-dependence of the response operator $\hat{K}$ (see Eqs. (11)–(13)). It disappears in a conventional continuum approach. Its magnitude, as observed for the model solute, proved to be extremely large (the difference in λ values for cations and anions reached 30 kcal/mol) [46]. In the present study of real chemical objects we expected to find it significantly reduced.

Table 1
Reorganization energies λ (in kcal/mol) for ion-radicals of structures A and B in water

The ionic form	System A		System B
	AM1[a]	Ab initio[a]	Ab initio
Anion	37.6	32.4	38.1
Cation	31.9	24.8	33.9
Antianion	32.4	28.2	35.1

[a] Both semiempirical and ab initio charge distributions were considered, see Section 3.4.

The computational results are listed in Table 1 ($T = 300$ K). The discrepancy of λ's between cations and anions reduces to a reasonable value 6–8 kcal/mol. This is a result of a significant charge delocalization over bulky donor and acceptor centers. It can be also argued that for intramolecular ET systems considered in the present work the solute charges are significantly screened from the approach of solvent dipoles, contrary to the model case of strongly separated dumbbell centers, considered earlier. The charge distribution changes not quite symmetrically from an anionic to a cationic solute, i.e. the absolute values of atomic charges are not the same, whereas this was exactly so for the model two-site solute. This symmetry of electronic structures was distorted in a course of a quantum-chemical computation, the details of which were different for cations and anions. It was regenerated by performing a "pure experiment" which considered the "antianions" of structures A and B, i.e. the corresponding cationic substrates with those charge distributions ρ_I and ρ_{II} for each of them obtained from the anionic distributions by a straightforward inversion of the charge sign. For such idealized case the continuum theory predicts the same λ as for the parent anion. The observed discrepancy of λ's became even less in this purely symmetric test, but is significant enough as a demonstration of the nonlinear effect.

In the computations reported in this section we used SPC water as a model polar solvent. This approach is sufficient to demonstrate that the nonlinear effect in reorganization energies λ, namely, the discrepancy between λ's computed for cations and anions of the same substrate in the same solvent, reduces to a reasonable value (6–8 kcal/mol) when a real polyatomic ET substrates are considered rather then their oversimplified models. However, at this level we cannot directly compare the absolute λ values with the experimental data measured in organic solvents with lower polarity and different structural properties than those found in water. The differences between λ's for structures B and A (Table 1) is close to that reported in the experiment [50–52] and to the similar estimate obtained in continuum FRCM computations [12,17]. Obtaining the absolute λ values comprises a more delicate matter (Table 2). This may depend significantly on the LJ and other parameters involved in a simulation, and there is little reason to expect that accurate numbers can be derived without special tuning of a force field. The impact of a particular force field is illustrated by simulations with

Table 2
Solvation (ΔG_{solv}) and reorganization (λ) energies of the hole-transfer reaction in water ($T = 300$ K)

Systems	$-\Delta G_{solv}$ (kcal/mol)						λ (kcal/mol)		
	Reactant			Product			MD/FRCM[a]		FRCM[b]
	MD/FRCM[a]		FRCM[b]	MD/FRCM[a]		FRCM[b]			
	I[c]	II[c]		I[c]	II[c]		I[c]	II[c]	
Cation-radical A	46.6	48.7	43.8	49.1	51.3	47.3	24.8	25.1	27.7
Cation-radical B	44.9	45.2	44.3	43.9	49.2	47.7	33.9	35.1	35.3

[a] MD/FRCM with ab initio charges.
[b] FRCM scheme with PM3 CI/BO charges, see Section 4.1.
[c] GROMOS-96 (I) and GROMACS (II) LJ parameters used for the CH1, CH2 and CH3 aliphatic groups; the NPT ensemble.

GROMOS96 [56] and GROMACS [58,50] LJ parameters (columns I and II in Table 2). Note that GROMOS parametrization was successfully tested earlier in the MD/FRCM treatment of equilibrium solvation energies in water [47].

The computed λ values are sensitive to the choice of a solute charge distribution, see Table 1. The use of ab initio charges gives lower values in comparison with the AM1 charges. The former seems to be preferable.

The simulation using SPC water (Table 2) can be only compared with the continuum FRCM results. This procedure with PM3 charges was earlier calibrated to reproduce experimental data. The computations here represent primary tentative estimates of the magnitude for solvation and reorganization free energy effects for real organic solutes. In such sort of a simulation, using a model polar solvent (SPC water) becomes hardly relevant and we have to address to a particular medium where the λ value has been measured (Section 5).

4.2. The temperature dependence of λ

The temperature dependence of reorganization energies has been repeatedly issued in the recent literature [16,18,19,61]. The present methodology opens the way for its direct study beyond simplified models. The computation, however, is difficult as the effect is weak: the λ values change only by few kcal/mol in the temperature range where the water solvent remains liquid. The computational errors seemed to be comparable in magnitude with the effect under study despite our effort of performing the MD runs as accurate as possible.

Computations for four temperatures $T = 273$, 300, 323 and 350 K included both anionic and cationic forms of structure A. For the cation the temperature grid was then refined at lower T-range in order to get better resolution of the effect. Three different methods have been tried. The first one used the NVT ensemble with the size of its MD cell established in a preliminary NPT simulation at $T = 300$ K. The second method used the NVT ensemble where the number of water particles was varied with temperature in order to reproduce the temperature change of the water density [62]. Finally, the NPT ensemble was used in the third method.

For the anion with structure A the three temperature curves showed more or less smooth decrease in λ when temperature increased. The result is illustrated in Fig. 2(a) and (b) by NPT computations where the observed change was most regular. The accuracy limit of this simulation is seen from Fig. 2(b): the refinement of our standard trajectory step (2 fs was changed for 1 fs) modified significantly the shape of the T-dependence on the scale of this Figure. However, the general negative trend keeps the same. The conclusion for the

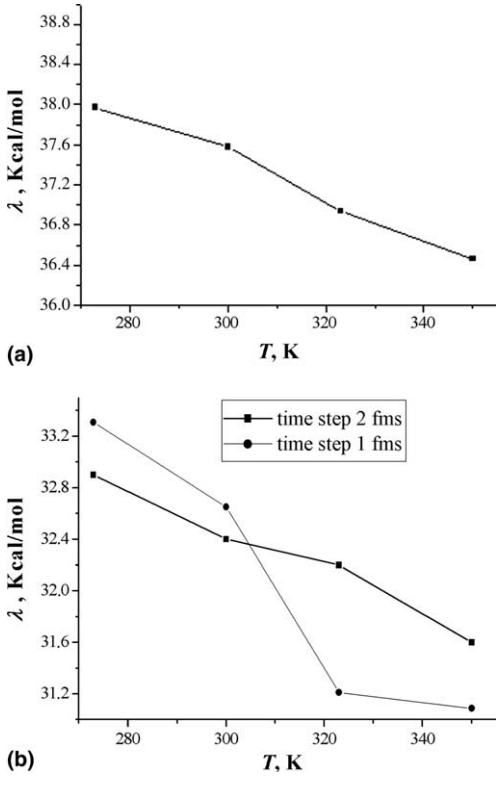

Fig. 2. The temperature dependence of reorganization energy $\lambda(T)$ computed by MD/FRCM for the anion-radical corresponding to structure A (NPT ensemble): (a) AM1 solute charges and (b) ab initio solute charges.

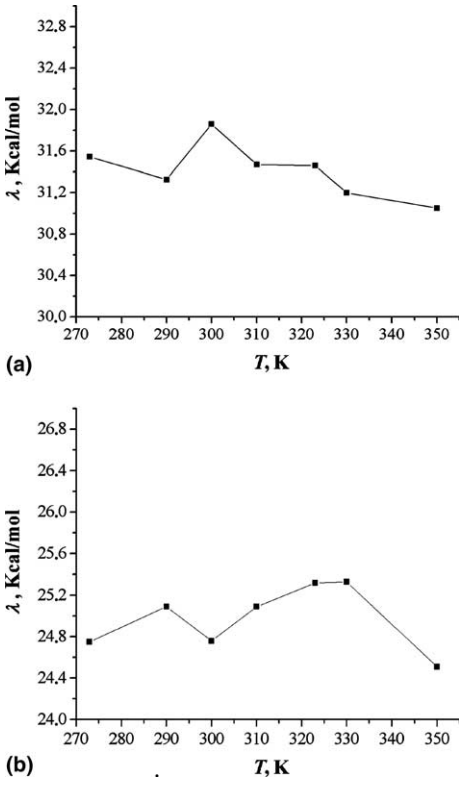

Fig. 3. The temperature dependence of reorganization energy $\lambda(T)$ computed by MD/FRCM for the cation-radical corresponding to structure A (NPT ensemble): (a) AM1 solute charges and (b) ab initio solute charges.

cation is not so definite (Fig. 3, the NPT ensemble) and both semiempirical and ab initio results can hardly be interpreted unambiguously as monotonic trends. The accuracy of a simulation is insufficient to resolve the slope of weak T-dependence at lower temperatures. The question whether the visible maximum reflects a real temperature effect remains open.

The understanding of the T-dependence of λ is complicated by the fact that it is influenced by several factors having different physical nature. Among them, except a manifestation of solvent dynamics, trivial T-dependence of the solvent density cannot be ignored [16,18]. Recent experiments [63] with exiplexes of 9-cyanophenantrene and aromatic electron donors in series of solvents of different polarity have demonstrated a doubtless correlation between temperature trends of their fluorescence spectra and the T-dependence of the solvent density. From a computational point of view this observation suggests that the choice of the solvent model used in a simulation (SPC water model in the present case) may essentially influence the final result.

The present calculations cannot be directly compared with the experiment. Experimentally, the temperature dependence of λ has been measured for a different organic solute in the non-water solvent (benzonitrile) [16,18,61]. Its interpretation [18] used a simplified molecular level model (the MSA) where a spherical shape is postulated for a solute particle. The monotonic temperature trend in Fig. 2(a) and (b) is the same as that observed in this work. It seems plausible to argue that a general character of temperature dependence of reorganization energies is similar for different substrates in a number of solvents. In order to get more definite conclusions one would have to repeat the similar MD/FRCM simulation for non-water solvents that was beyond the scope of the present study.

5. Intramolecular hole transfer in 1,2-dichloroethane

Recent models of non-water solvents related to the theme of the present work (DCE and tetrahydrofurane) are purely elaborated and additional technical problems, concerned with an application of MD/FRCM, also arise. The data collected in Table 3 illustrate the present situation for the case of cation-radicals A and B in DCE. Along with the reorganization energies the total solvation energies (i.e. the diagonal elements of the reorganization matrix including both inertial and inertialess polarization effects) are also listed. For reactant and product states their difference provides the solvation contribution to the ET reaction free energy. The MD/FRCM data are compared with continuum FRCM computations in which PM3-atomic charges were used.

Table 3
Solvation (ΔG_{solv}) and reorganization (λ) energies of the hole-transfer reaction in DCE ($T = 300$ K)

Systems	$-\Delta G_{solv}$ (kcal/mol)						λ (kcal/mol)			
	Reactant			Product			MD/FRCM[a]		FRCM[a]	Experiment
	MD/FRCM[a]		FRCM[a]	MD/FRCM[a]		FRCM[a]				
	I[b]	II[b]		I[b]	II[b]		I[b]	II[b]		
Cation-radical A	44.3	43.4 (44.3)[c]	37.8	44.9	41.8 (45.7)[c]	40.8	18.8	16.5 (16.7)[c]	10.4	12.2[d]
Cation-radical B	40.8	39.9	38.5	41.3	40.6	41.5	25.5	23.9	15.0	17.8

[a] MD/FRCM with ab initio charges and FRCM scheme with PM3 CI/BO charges see text.
[b] GROMOS-96 (I) and GROMACS (II) LJ parameters used for the CH1, CH2 and CH3 aliphatic groups; the NVT ensemble.
[c] Computed with Merz–Kolman solute charges.
[d] The extrapolated value [51], see the text.

This last method was specially calibrated [12,15] in order to reproduce both solvation and ET reorganization energies in different solvents and, with poor experimental information, it provides an independent implicit evidence for a purpose of comparison.

The simulation in DCE provides a comparison with the existing experiment [50,51]. (Note, however, that the direct experimental measurement of λ has not been reported. The solvent reorganization energies were extracted in terms of the complicated multi-parameter procedure [50,52] fitting the Golden Rule rate expression to the observed ET rate constants). With this reservation, one can see (Table 3) that MD/FRCM treatment has predicted reasonable but exaggerate values of λ. This is not a consequence of improper LJ parameters. We tested two different parameter sets for solute atomic groups involving combinations of C and H atoms (columns I and II of Table 3) with no significant effect on the resulted λ-values. Moreover, in the recently elaborated refined force field [64] the same parameters were found to be confined between their GROMOS (column I) and GROMACS (column II) values, so even invoking this new scheme would not change the results.

In order to check how important are the details of a solute charge distribution, the computations for structure A was repeated with Merz–Kolman solute charges used instead of ESP charges implemented in all other computations (see Section 3.4 and [54]). The results have not changed significantly (Table 3). Therefore, it seems that in order to get better agreement with the experiment within the MD/FRCM scheme, one has to modify the DCE charge distribution recommended earlier [60]. Implicitly, this guess is also confirmed by the observation that MD/FRCM and continuum FRCM computations of λs give much closer results in water (a perfectly calibrated solvent, Table 2), than in DCE (Table 3). Note that the calibration of parameters in [60] was not addressed for computations of solvation free energies in DCE. According to the recent experience [64], special tuning of charges is necessary for such purpose.

6. Conclusion

As a development of earlier studies [46,47] we elaborated and performed computationally the new method of treating electronic polarization of a solvent in the framework of MD simulations of solvation effects (the MD/FRCM method) using the nonpolarizable models. The method provides a physically relevant background for separating the inertial and inertialess components of polarization fields, the necessary step in theoretical studies of ET reactions. First computations of outer-sphere reorganization energies (speaking exactly, their electrostatic component) for intramolecular ET in real polyatomic solutes are performed. It is shown that:

- MD/FRCM treats with an acceptable accuracy ET reorganization energies in biphenylyl-spacer-naphtyl systems. The calculated absolute λ values are reasonable for both cation- and anion-radical systems and, if necessary, they can be further corrected by improving force field parametrizations;
- The calculated temperature dependence of λ for the anion-radical substrate is qualitatively the same as that described in the previous works [16,18,61] and interpreted there within the MSA approach;
- The use of AM1 and ab initio geometries and charges for description of solutes leads to similar values of computed λ's but the ab initio results giving lower values seem preferable. The absolute λ values are sensitive to the choice of a solute charge distribution and, probably, it is including the effect of the SCRF polarization of the diabatic ET states which mainly accounts for the advantage of the ab initio charges. In choosing these particular quantum-chemical methods we based on the experience of the earlier continuum-level ([12,15]; semiempirical charges) and molecular-level ([46,47] and [65,66]; both semiempirical and ab initio charges) computations. In the case of ab initio computations the basis sets implemented seemed to provide an acceptable optimum between the accuracy and the computational cost of a calculation;
- We investigated the effect which, being essentially nonlinear, is missing in conventional dielectric continuum approaches. It has been revealed [46] as different values of λ in cationic and anionic substrates originated from the same parent neutral molecular structure. Its value reaches several kcal/mol for real ET substrates according to the computations performed in the present work, much smaller than in the model two-site system studied earlier [46]. A dipolar two-site substrate, frequently used as a model for real substrates in MD simulations of the solvation phenomena [67–69], in particular, for description of intramolecular ET [45,46,70], overestimates significantly the nonlinearity effects in λ.

The first attempt of a computation of the hole transfer in DCE (Table 3) showed, provided the experimental λ values [51] are sufficiently accurate, that our approach with the existing parametrization (not addressed to free energy simulations) overrates reorganization energies by $\sim$5 kcal/mol. The defect of this magnitude could be eliminated by proper tuning solvent parameters. Simulations of the temperature dependence at this level of sophistication are premature in our opinion. As simulation in water showed, the effect is extremely weak so that the present purely elaborated models of organic solvents

could hardly reveal its real features. Further applications require the extention of the MD/FRCM techniques and its parametrization for such systems.

Acknowledgement

IVL, AVT, MVV and MVB thank the Russian Foundation of Fundamental Research (Project No. 02-03-33049 and 05-03-33015) for financial support.

References

[1] J. Tomasi, M. Persico, Chem. Rev. 94 (1994) 2027.
[2] C.J. Cramer, D.G. Truhlar, Chem. Rev. 99 (1999) 2161.
[3] J. Tomasi, R. Cammi, B. Mennucci, C. Cappelli, S. Corni, Phys. Chem. Chem. Phys. 4 (2002) 5697.
[4] F. Javier Luque, C. Curutchet, J. Munoz-Muriedas, A. Bidon-Chanal, I. Soteras, A. Morreale, J.L. Gelpi, M. Orozco, Phys. Chem. Chem. Phys. 5 (2003) 3827.
[5] G.N. Chuev, M.V. Basilevsky, Usp. Chim. 72 (2003) 827 (English version: G.N. Chuev, M.V. Basilevsky, Russ. Chem. Rev. 72 (2003) 735).
[6] R.A. Marcus, N. Sutin, Biochem. Biophys. Acta 811 (1985) 265.
[7] M.V. Basilevsky, G.E. Chudinov, M.D. Newton, Chem. Phys. 179 (1994) 263.
[8] Y.-P. Liu, M.D. Newton, J. Phys. Chem. 99 (1995) 12382.
[9] M.V. Basilevsky, G.E. Chudinov, I.V. Rostov, Y.-P. Liu, M.D. Newton, J. Mol. Structr. – THEOCHEM 371 (1996) 191.
[10] I.V. Kurnikov, L.D. Zusman, M.G. Kurnikova, R.S. Farid, D.N. Beratan, J. Am. Chem. Soc. 119 (1997) 5690.
[11] K. Kumar, I.V. Kurnikov, D.N. Beratan, D.H. Waldeck, M.B. Zimmt, J. Phys. Chem. A 102 (1998) 5529.
[12] M.V. Basilevsky, I.V. Rostov, M.D. Newton, Chem. Phys. 232 (1998) 189;
M.D. Newton, I.V. Rostov, M.V. Basilevsky, Chem. Phys. 232 (1998) 201.
[13] E.L. Mertz, V.A. Tikhomirov, L.I. Krishtalik, J. Phys. Chem. A 101 (1997) 3433.
[14] E.L. Mertz, E.D. German, A.M. Kuznetsov, L.I. Krishtalik, Chem. Phys. 215 (1997) 355.
[15] I.V. Rostov, M.V. Basilevsky, M.D. Newton, in: L.G. Pratt, G. Hummer (Eds.), Simulation of Electrostatic Interactions in Solution, AIP, New York, 1999, p. 331.
[16] M.B. Zimmt, D.H. Waldeck, J. Phys. Chem. A 107 (2003) 3580.
[17] I.V. Leontyev, M.V. Basilevsky, M.D. Newton, Theor. Chem. Acc. 111 (2004) 110.
[18] P. Vath, M.B. Zimmt, D.V. Matyushov, G.A. Voth, J. Phys. Chem. B. 103 (1999) 9130.
[19] D.V. Matyushov, J. Chem. Phys. 120 (2004) 7532.
[20] M. Marchi, J.N. Gehlen, D. Chandler, M. Newton, J. Am. Chem. Soc. 115 (1993) 4178.
[21] I. Muegg, P.X. Qi, A.J. Wand, Z.T. Chu, A. Warshel, J. Phys. Chem. B 101 (1997) 825.
[22] L.W. Ungar, M.D. Newton, G.A. Voth, J. Phys. Chem. B 103 (1999) 7367.
[23] H. Sato, F. Hirata, J. Phys. Chem. A 106 (2002) 2300;
H. Sato, Y. Kobori, S. Tero-Kabota, F. Hirata, J. Chem. Phys. 119 (2003) 2753;
H. Sato, Y. Kobori, S. Tero-Kabota, F. Hirata, J. Phys. Chem. B 108 (2004) 11709.
[24] S.I. Pekar, Untersuchungen über Die Electronentheorie Der Kristalle, Akademic Verlag, Berlin, 1954.
[25] M.A. Vorotyntsev, A.A. Kornyshev, Electrostatics of Media with the Spatial Dispersion, Nauka, Moscow, 1993.
[26] A.A. Kornyshev, in: R.R. Dogonadze, E. Kalman, A.A. Kornyshev, J. Ulstrup (Eds.), The Chemical Physics of Solvation, Part A, Elsevier, Amsterdam, 1986, p. 77.
[27] R.R. Dogonadze, A.A. Kornyshev, A.M. Kuznetsov, Theor. Math. Phys. 15 (1973) 127 (in Russian).
[28] M.A. Vorotyntsev, J. Phys. C: Solid State Phys. 11 (1978) 3323.
[29] M.V. Basilevsky, D.F. Parsons, J. Chem. Phys. 105 (1996) 3734.
[30] M.A. Kuznetsov, J. Ulstrup, M.A. Vorotyntsev, in: R.R. Dogonadze, E. Kalman, A.A. Kornyshev, J. Ulstrup (Eds.), The Chemical Physics of Solvation, Part C, Elsevier, Amsterdam, 1986, p. 163.
[31] A.A. Kornyshev, A.M. Kuznetsov, D.K. Phelp, M.J. Weaver, J. Chem. Phys. 91 (1989) 7159.
[32] A.A. Kornyshev, A.I. Rubinshtein, M.A. Vorotyntsev, J. Phys. C: Solid State Phys. 11 (1978) 3307.
[33] S.W. Rick, S.J. Stuart, B.J. Berne, J. Chem. Phys. 101 (1994) 6141.
[34] S.J. Stuart, B.J. Berne, J. Phys. Chem. 100 (1996) 11934.
[35] S.W. Rick, B.J. Berne, J. Phys. Chem. B 101 (1997) 10488.
[36] S.W. Rick, J. Chem. Phys. 114 (2001) 2276.
[37] G.A. Kaminski, H.A. Stern, B.J. Berne, R.A. Friesner, Y.X.X. Cao, R.B. Murphy, R. Zhou, T.A. Halgren, J. Comp. Chem. 23 (2002) 1515.
[38] M. Neumann, O. Steinhauser, Chem. Phys. Lett. 106 (1984) 563.
[39] D. Levesque, J.J. Weis, G.N. Patey, Mol. Phys. 51 (1984) 333.
[40] S.T. Russell, A. Warshel, J. Mol. Biol. 185 (1985) 389.
[41] J.A.C. Rullmann, P.T. van Duijnen, Mol. Phys. 63 (63) (1988) 451.
[42] P. Ahlström, A. Wallqvist, S. Engström, B. Jönsson, Mol. Phys. 68 (1989) 563.
[43] M. Sprik, M.L. Klein, J. Chem. Phys. 89 (1988) 7556.
[44] M. Sprik, M.L. Klein, K. Watanabe, J. Phys. Chem. 94 (1990) 6483.
[45] K. Ando, J. Chem. Phys. 106 (1997) 116;
K. Ando, J. Chem. Phys. 114 (2001) 9040;
K. Ando, J. Chem. Phys. 114 (2001) 9470.
[46] I.V. Leontyev, M.V. Vener, I.V. Rostov, M.V. Basilevsky, M.D. Newton, J. Chem. Phys. 119 (2003) 8024.
[47] M.V. Vener, I.V. Leontyev, M.V. Basilevsky, J. Chem. Phys. 119 (2003) 8038.
[48] H.J.C. Berendsen, J.P.M. Postma, W.F. van Gunsteren, J. Hermans, in: B. Pullman, D. Reidel, Intermolecular Forces, Dordrecht, 1981, p. 331.
[49] M.V. Vener, I.V. Leontyev, Yu.A. Dyakov, M.V. Basilevsky, M.D. Newton, J. Phys. Chem. B 106 (2002) 13078.
[50] G.L. Closs, L.T. Calcaterra, N.J. Green, K.W. Penfield, J.R. Miller, J. Phys. Chem. 90 (1986) 3673.
[51] M.D. Johnson, J.R. Miller, N.S. Green, G.L. Closs, J. Phys. Chem. 93 (1989) 1173.
[52] G.L. Closs, J.R. Miller, Science 240 (1988) 440.
[53] M.V. Basilevsky, G.E. Chudinov, D.V. Napolov, L.M. Timofeeva, Chem. Phys. 173 (1993) 345.
[54] M.J. Frisch, G.W. Trucks, H.B. Schlegel, et al., Gaussian-03 (Revision B.03), Gaussian Inc., Pittsburgh, PA, 2003.
[55] C.M. Breneman, K.B. Wiberg, J. Comp. Chem. 11 (1990) 361.
[56] W.F. van Gunsteren, S.R. Billeter, A.A. Eising et al., Biomolecular Simulation: The GROMOS96 Manual and User Guide, vdf Hochschulverlag AG an der ETH Zürich and BIOMOS b.v.: Zürich, Groningen, 1996.
[57] I.G. Tironi, R. Sperb, P.E. Smith, W.F. van Gunsteren, J. Chem. Phys. 102 (1995) 5451.
[58] H.J.C. Berendsen, D. van der Spoel, R. van Drunen, Comp. Phys. Commun. 91 (1995) 43.
[59] E. Lindahl, B. Hess, D. van der Spoel, J. Mol. Mod. 7 (2001) 306.

[60] I. Benjamin, J. Chem. Phys. 97 (1992) 1432.
[61] P. Vath, M.B. Zimmt, J. Phys. Chem. A 104 (2000) 2626.
[62] G.S. Kell, J. Chem. Eng. Data 20 (1975) 97.
[63] M.G. Kuźmin, E.V. Dolotova, I.V. Soboleva, Russ. J. Phys. Chem. 76 (2002) 1109.
[64] C. Oostenbrink, A. Villa, A.E. Mark, W.F. van Gunsteren, J. Comput. Chem. 25 (2004) 1656.
[65] M. Kawata, S. Ten-no, S. Kato, F. Hirata, Chem. Phys. 203 (1996) 53.
[66] W.L. Jorgensen, BOSS, Version 4.2. Biochemical and Organic Simulation System. User's Manual for Unix, Linux and Windows, Yale University, New Haven Connecticut, 2000.
[67] P.V. Kumar, M. Maroncelli, J. Chem. Phys. 103 (1995) 3038.
[68] G.S. Del Buono, F.E. Figuirido, R.M. Levy, Chem. Phys. Lett. 263 (1996) 521.
[69] S. Nugent, B.M. Ladanyi, J. Chem. Phys. 120 (2004) 874.
[70] R.M. Levy, M. Belhadj, D.B. Kitchen, J. Chem. Phys. 95 (1991) 3627.